Geophysical Journal International

Geophys. J. Int. (2011) **184,** 541–554 doi: 10.1111/j.1365-246X.2010.04873.x

Continent–ocean-transition across a trans-tensional margin segment: off Bear Island, Barents Sea

Wojciech Czuba,[1] Marek Grad,[2] Rolf Mjelde,[3] Aleksander Guterch,[1] Audun Libak,[3] Frank Krüger,[4] Yoshio Murai,[5] Johannes Schweitzer[6] and the IPY Project Group

[1] *Institute of Geophysics Polish Academy of Sciences, Ks. Janusza* 64, 01-452 *Warsaw, Poland. E-mail: wojt@igf.edu.pl*
[2] *Institute of Geophysics, University of Warsaw, Pasteura* 7, 02-093 *Warsaw, Poland*
[3] *Department of Earth Science, Allegt.* 41, 5007 *Bergen, Norway*
[4] *Department of Geosciences, University of Potsdam, Karl-Liebknecht Strasse* 24, 14476 *Potsdam, Germany*
[5] *Institute of Seismology and Volcanology, Hokkaido University,* N10S8 *Kita-Ku Sapporo* 060-0810, *Japan*
[6] *NORSAR, Gunnar Randers vei* 15, N-2007 *Kjeller, Norway*

Accepted 2010 October 27. Received 2010 October 25; in original form 2010 January 12

SUMMARY

A 410 km long Ocean Bottom Seismometer profile spanning from the Bear Island, Barents Sea to oceanic crust formed along the Mohns Ridge has been modelled by use of ray-tracing with regard to observed *P*-waves. The northeastern part of the model represents typical continental crust, thinned from *ca*. 30 km thickness beneath the Bear Island to *ca*. 13 km within the Continent–Ocean-Transition. Between the Hornsund FZ and the Knølegga Fault, a 3–4 km thick sedimentary basin, dominantly of Permian/Carboniferous age, is modelled beneath the *ca*. 1.5 km thick layer of volcanics (Vestbakken Volcanic Province). The *P*-wave velocity in the 3–4 km thick lowermost continental crust is significantly higher than normal (*ca*. 7.5 km s^{-1}). We interpret this layer as a mixture of mafic intrusions and continental crystalline blocks, dominantly related to the Paleocene-Early Eocene rifting event. The crystalline portion of the crust within the south-western part of the COT consists of a *ca*. 30 km wide and *ca*. 6 km thick high-velocity (7.3 km s^{-1}) body. We interpret the body as a ridge of serpentinized peridotites. The magmatic portion of the ocean crust accreted along the Knipovich Ridge from continental break-up at *ca*. 35 Ma until *ca*. 20 Ma is 3–5 km thicker than normal. We interpret the increased magmatism as a passive response to the bending of this southernmost part of the Knipovich Ridge. The thickness of the magmatic portion of the crust formed along the Mohns Ridge at *ca.* 20 Ma decreases to *ca.* 3 km, which is normal for ultra slow spreading ridges.

Key words: Controlled source seismology; Dynamics of lithosphere and mantle; Crustal structure; Atlantic Ocean.

INTRODUCTION

The development of the sheared continental margins of the western Barents Sea continental platform, rifting and subsequent seafloor spreading are processes which form the face of our planet. The subject of the paper are results of investigations along a seismic wide-angle reflection and refraction profile made within the 4th International Polar Year (IPY) in the frame of the international project 'The Dynamic Continental Margin Between the Mid-Atlantic-Ridge (Mohns Ridge, Knipovich Ridge) and the Bear Island Region'. Apart of seismic refraction investigations the project contains seismic reflection profiling, installation of 3 broadband seismic stations on Bear Island, Hopen and southern Spitsbergen, as well as one year deployment of 12 broadband OBSs (Schweitzer *et al*. 2008; Wilde-Piórko *et al*. 2009; Pirli *et al*. 2010).

The 410 km long profile BIS-2008 (Bear Island—South) crossing the trans-tensional Vestbakken Volcanic Province and the boundary between oceanic crust of the Northern Atlantic and continental crust of the Barents Sea continental platform (Fig. 1) was performed in 2008 August. Previously this region has been studied by geophysical surveys, including active and passive seismic experiments, gravity and magnetic (e.g. Vogt e*t al.* 1981; Klingelhöfer *et al.* 2000a,b; Breivik *et al.* 2003). The continent–ocean boundary (COB) in the region between Svalbard in the north and Scandinavia in the south has been relatively well studied by use of multichannel reflection seismics—for review see for example, Gabrielsen *et al*. (1990) and Faleide *et al*. (2008). Deep seismic soundings with use of the refraction technique generally provide information about the crystalline basement and crust-mantle transition (e.g. Davydova *et al*. 1985; Faleide *et al.* 1991; Sellevoll *et al.* 1991; Mjelde *et al.* 2002; Ljones *et al*. 2004; Czuba *et al*. 2008). This has led to important knowledge on the lithospheric structure, the hydrocarbon potential and parts of the tectonic and sedimentary dynamics. These studies have also shown that a complete understanding of continental margins is

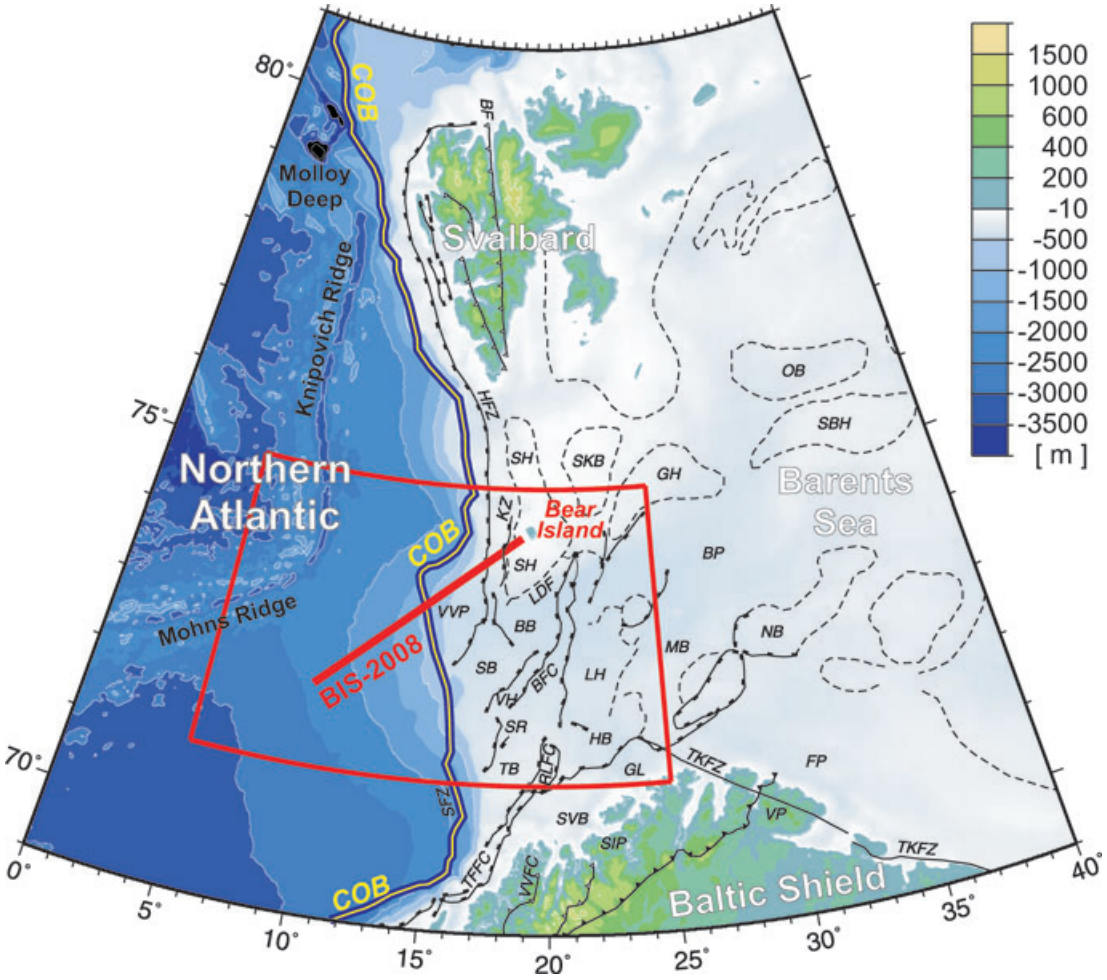

Figure 1. Location map of the BIS-2008 seismic profile (Mohns Ridge-Bear Island) on the background of topography/bathymetry map (Jakobsson *et al.* 2000) and simplified tectonic elements (Gabrielsen *et al*. 1990; Faleide *et al*. 2008) of the continental margin in the area of the Northern Atlantic (Norwegian-Greenland Sea). COB, continent-ocean boundary (from interpretation of gravity data, Breivik *et al.* 1999); main fault zones and basins: BB, Bjørnøya Basin; BF, Billefjorden Fault; BP, Bjarmeland Platform; BFC, Bjørnøyrenna Fault Complex; FP, Finnmark Platform; GH, Gardarbanken High; HB, Hammerfest Basin; HFZ, Hornsund Fault Zone; KF, Knølegga Fault; LDF, Leirdjupet Fault; LH, Loppa High; NB, Nordkapp Basin; OB, Olga Basin; SB, Sørvestsnaget Basin; SBH, Sentralbanken High; SH, Stappen High; SKB, Sørkap Basin; SFZ, Senja Fracture Zone; SR, Senja Ridge; TFFC, Tromsø-Finnmark Fault Complex; TB, Tromsø Basin; TKFZ, Trollfjord-Komagelv Fault Zone; VH, Veslemøy High; VP, Varanger Platform; VVP, Vestbakken Volcanic Province. The red frame is an area of Fig. 2 where details of the profile are shown.

only possible when also the deeper crustal and mantle architecture beneath the margins is imaged. Our study represents the first wide-angle seismic study across the Vestbakken Volcanic Province, which sub-basalt structures are unknown. It is assumed that the province was dominantly formed in response to the initial opening of the Norwegian-Greenland Sea in Early Eocene (Faleide *et al.* 1988).

TECTONIC SETTING

The Barents Sea region has an intracratonic setting. It has been affected by several phases of tectonism since the Caledonian Orogeny (Talwani & Eldholm 1977; Birkenmajer 1981). Structurally, the Barents Sea continental shelf is dominated by ENE–WSW to NE–SW and NNE–SSW to NNW–SSE trends. The western part of the Barents Sea has been the tectonically most active sector during Mesozoic and Cenozoic times (Gabrielsen *et al.* 1990). The area of Bjørnøya (Bear Island) was influenced by large-scale block faulting in Late Devonian to Early Carboniferous times (Gjelberg 1981, 1987). In the western part of the Barents Sea area there was localized magmatic activity during Palaeocene and Eocene probably related to the break-up of the North Atlantic, starting with regional dextral shear in the Early Palaeocene and continuing with rifting from 36 Ma ago (Talwani & Eldholm 1977; Myhre *et al.* 1982; Eldholm *et al.* 1987).

The evolution of the North Atlantic Ocean can be divided into two main stages. During the first stage in the Early Eocene continental break-up occurred and sea floor spreading started along the Reykjanes, Aegir and Mohns Ridges (Talwani & Eldholm 1977). This spreading was coupled to spreading along the Gakkel-Nansen Ridge in the Arctic Ocean through the sheared western Svalbard margin—comprising the Senja, Greenland and Hornsund Fracture Zones (Talwani & Eldholm 1977; Sundvor & Eldholm 1979; Lundin & Doré 2002; Mjelde *et al.* 2002; Mosar *et al.* 2002; Ljones *et al.* 2004; Døssing *et al.* 2008). The shearing along north-northwest trending faults between Svalbard and northeast Greenland and the resulting transpression created the Spitsbergen fold and thrust belt to the north. Conversely, transtension caused thinning and weakening of the crust and dense mantle material was intruded most significantly at the Vestbakken Volcanic Province (Sundvor & Eldholm 1979; Eiken & Austegard 1987; Eldholm *et al.* 1987).

A change in the spreading direction from NNW–SSE to NW–SE and the following termination of the Western Spitsbergen Orogeny marks the beginning of the second stage of North Atlantic evolution. This started in Early Oligocene when spreading in the Labrador sea ceased (Talwani & Eldholm 1977; Mosar *et al.* 2002). The beginning of the stage unlocked the northward development of the Mid Atlantic Ridge. The spreading axis propagated into the Spitsbergen Shear Zone creating the asymmetric, ultraslow and obliquely spreading Knipovich Ridge. Around 23 Ma ago spreading started along the Molloy Ridge and around 10 Ma ago continental break-up occurred along the Fram Strait establishing connection between the Arctic and the Northern-Atlantic Ridges (Crane *et al.* 1991; Lundin & Doré 2002).

SEISMIC DATA ACQUISITION AND PROCESSING

The seismic refraction experiment between Mohns Ridge and Bear Island was done in 2008 August with use of two ships: Norwegian *R/V Håkon Mosby* and Polish *R/V Horyzont II*. Geographical coordinates of BIS-2008 profile are: $\varphi_0 = 72.114^\circ$N, $\lambda_0 = 9.600^\circ$E (southwesternmost airgun shot); $\varphi_{end} = 74.460^\circ$N, $\lambda_{end} = 19.263^\circ$E (northeasternmost land station; see Figs 1 and 2). The sources of seismic waves were airgun and TNT shots performed in the sea. Offshore airgun shooting along the whole profile length, was done by *R/V Håkon Mosby* with use a system of four airguns of 1200 in^3 each and total volume of 4800 in^3 (78.66 l). Altogether 1914 airgun shots were performed with distance interval of 200 m (corresponding to 1 min time interval), at the depth of approximately 10 m. A total of 104 TNT shots (25 kg of TNT each) were done by *R/V Horyzont II* along the northeastern part of the profile (distance along profile 176.4–385.5 km), with average interval of 2 km. Firing depth of the TNT explosions was approximately 30 m.

R/V Håkon Mosby deployed 15 short-period, three-component, digital ocean bottom seismometers (OBS), which were maintained by the Norwegian-Japanese team (station numbers 0102–0115). In the investigated area 12 DEPAS broadband German OBSs were deployed in 2007 September by *R/V Horyzont II* which operated in the long-term passive experiment. The data from two inline OBSs (0008 and 0011) were included into BIS-2008 profile data set (Fig. 2) but they were excluded from the modelling because of relatively low data quality. At Bear Island, vertical-component 'RefTek 125 Texan' stations with 4.5 Hz geophones were deployed by the Polish team with use of *R/V Horyzont II* in four places in the southern and eastern parts of the island. We used also records from 13 LE3D stations with 3-component, 5 s corner period Lenartz seismometers (0020–0033) from the northern and central parts of the island installed by the Institute of Geosciences, University of Potsdam, Germany team to study local and regional seismicity. For detailed location of land stations see inset in Fig. 2.

Location determination and synchronization of all shots and seismic receivers were obtained using satellite GPS system. All stations (OBSs and land stations) recorded continuously during the experiment. The sampling rate was 0.004 s (250 Hz) for short period OBSs, 0.01 s (100 Hz) for 'RefTek 125 Texans', 0.008 s (125 Hz) for LE3D stations and 0.05 s (20 Hz) for broadband OBSs. Data from short period OBSs were digitised from analogue tapes and cut to 60 s record length and tied to the navigation. All the data were then resampled to 0.01 s (100 Hz). In the pre-processing all

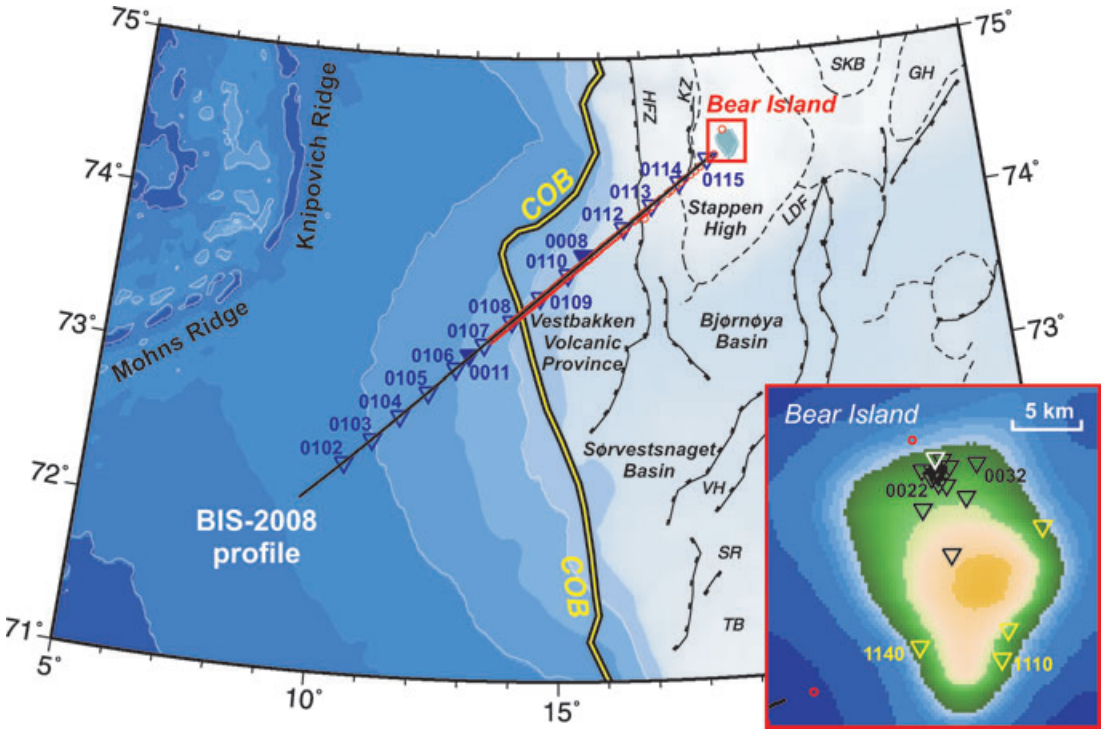

Figure 2. Location map with details of the BIS-2008 seismic profile. Blue open triangles are short period OBSs with their numbers (0102–0115); blue filled triangles are broadband DEPAS OBSs with their numbers (0008 and 0011). Seismic land stations at Bear Island are shown in insert: the small aperture array of 13 short period LE3D stations (0020–0039 marked by black triangles) and the location of 4 'RefTek 125 Texan' stations with 4.5 Hz geophones (1110–1140 marked by yellow triangles). The white triangle shows the location of the permanent broadband station at Bear Island. Red dots show locations of 104 TNT shots with average distance interval 2 km, and black dots show 1914 airgun shots with distance interval of 200 m. For abbreviations of main fault zones and basins see Fig. 1.

recordings were cut into single 60 s long time windows, with 'zero' time in original shot time. Twelve OBSs recorded successfully during the whole experiment and one (OBS0106) recorded only part of the data. During processing and interpretation a band-pass filter of 3–17 Hz was usually used.

The use of different sources and recorders gives an unique opportunity to evaluate them, compare data quality and optimise the wide-angle seismic technique in margin settings. The examples of record sections are shown in Figs 3–6. The data quality is generally very good. The next three figures show record sections (Figs 4–6) together with traveltimes calculated for the crustal velocity model (Fig. 7), which was derived using a ray tracing technique from all the data available. Most of OBSs revealed clear arrivals for airgun shots beyond 100 km and even 150–200 km for TNT shots. Land stations at the Bear Island were located inside a relatively small area, so we expected very similar records (see insert in Figs. 2, 5 and 6). However, we observed significantly different data quality. The best stations were located far away from the sea, while coastal stations were noisy because of sea water noise and strong winds.

The advantage of airgun shots is their density. Short distance between shots (in this case 200 m) permit 'continuous' correlation of phases. Offset up to 50–100 km is sufficient for the thin oceanic crust. The distance between TNT shots is much larger (in this case about 2 km) and permit correlation of the envelope of consecutive phases. However, because of much larger energy the recorded onsets are visible up to 200 km and are of great importance for mapping the continental lower crust and crust–mantle transition. For both types of source (airgun and TNT) short period recorders (both OBSs and land stations) are preferred. So, in the case of seismic refraction study in the ocean–continent transition we recommend short period recorders, dense coverage of the airgun shots in the thin oceanic crust area and TNT shots for recognition of the thick continental crust.

SEISMIC WAVE FIELD

In general, the seismic records obtained along BIS-2008 profile are of good-quality allowing detailed wave field analysis and

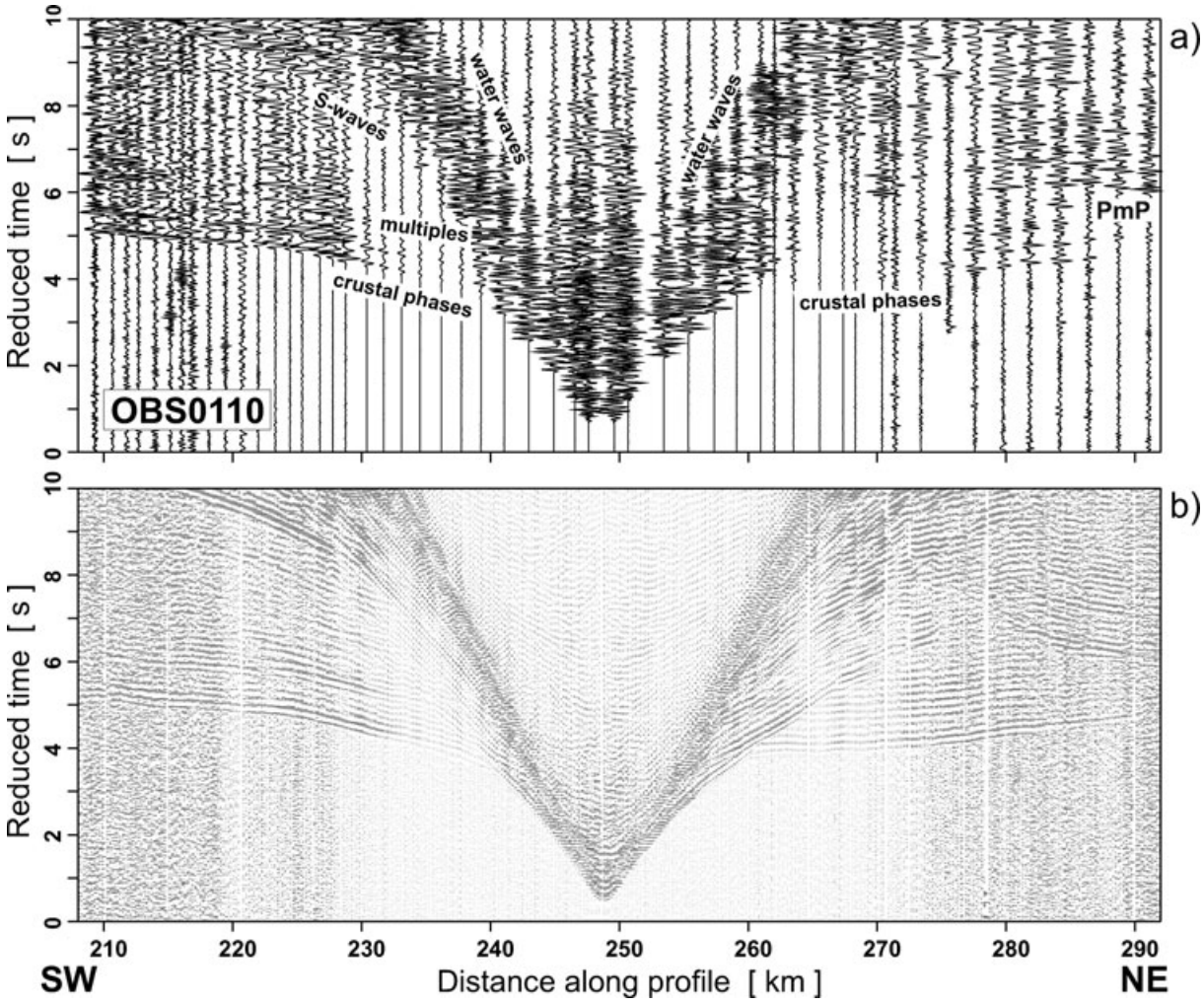

Figure 3. Comparison of amplitude-normalized, vertical-component seismic sections obtained by different sources. All examples are for OBS0110, band-pass filtration is 3–17 Hz and velocity reduction 8 km s^{-1}. (a) TNT shots, wiggle trace (WT) plot, ampl = 1.5; (b) airgun records, all traces are plotted, variable area (VA) plot, ampl = 0.75. VA plot is best to show the correlation of phases and is preferred for the correlation process and kinematic modelling. On the other hand WT plots show true relative amplitudes and were used in dynamic modelling, when observed and calculated amplitudes were compared. Note characteristic strong phases recorded in oceanic part of profile-–water waves (direct and multiples) which contain most of energy, relatively weak *P*-waves in the crust and uppermost mantle, multiples and S-phases.

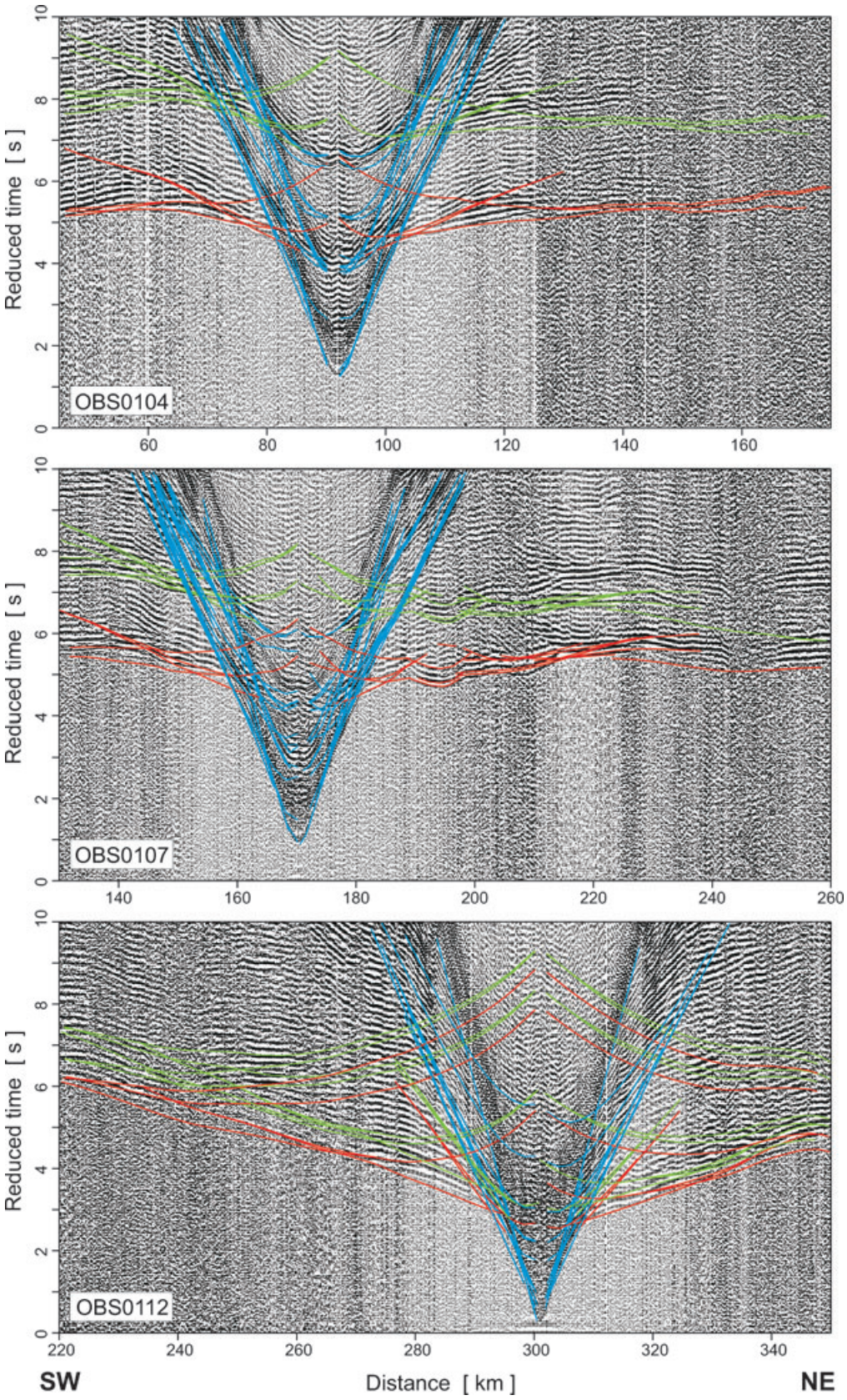

Figure 4. Examples of the 2-D seismic modelling along BIS-2008 profile for OBS0104, OBS0107 and OBS0112. VA plots of normalized experimental record sections (vertical-component) from airgun shots are shown with calculated traveltimes for the final model of the structure: blue lines—traveltimes of water waves and waves in low velocity sediments (including multiples), red lines—traveltimes of crustal *P*-waves and waves reflected and refracted from the Moho, green lines—traveltimes of waves with one extra reflection in water layer. Band-pass filtration is 3–17 Hz and velocity reduction 8 km s^{-1}. For the final model of the structure see Fig. 9.

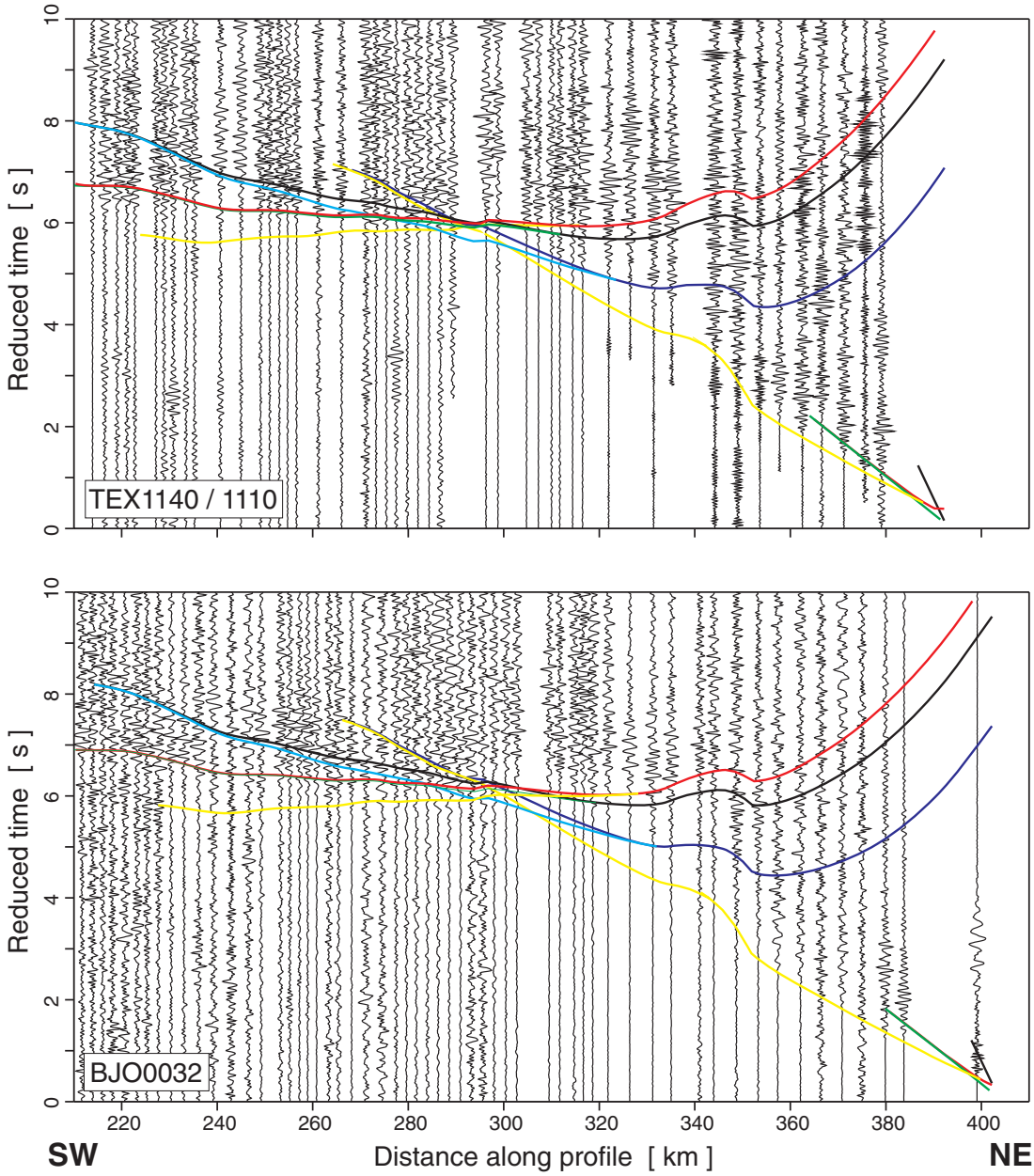

Figure 5. Examples of the 2-D seismic modelling along BIS-2008 profile for two land stations at Bear Island: upper section (vertical-component) is a combination of TNT shots recorded at 'RefTek 125 Texan' stations TEX1140 and TEX1110 from the southern part of island and the lower section (vertical-component) shows records of the short period LE3D station BJO0032 in the northern part of island. Note distant crustal and Pn phases (offset 100–190 km from the source): Pn at distance 270–300 km (with calculated traveltime almost horizontal line in yellow), middle crust phase at distance 250–290 km (with calculated traveltime line in blue) and lower crust high velocity phase at distance 210–260 km (with calculated traveltime line in red). Band-pass filtration is 3–17 Hz and velocity reduction 8 km s^{-1}. For the final model of the structure see Fig. 7.

crustal structure modelling to be made. An example of amplitude-normalized seismic section of TNT shots recorded by OBS0110 is shown in Fig. 3. Waves from the crust and uppermost mantle recorded in oceanic part of the profile are much weaker than water waves. The phase identification is complicated by relatively strong reverberations (e.g. Figs 3, 4, 6) and considerable amount of noise in some places (very noisy traces were removed manually from the sections). During the next steps of the data interpretation, particularly during correlation of seismic phases, various plot methods and visualisations were used. Band-pass filters, zooms and change in amplification were applied to different parts of record sections to extract and display the clearest signal arrivals, which made arrival time picking more accurate. Sixteen crustal and 3 sediment phases were identified and picked. Fig. 3 shows a comparison between the TNT and airgun sources for the OBS0110.

Examples of the wave field together with calculated traveltimes for the model of the structure are shown in Figs 4–6. We can observe significant differences between the southwestern and northeastern parts of profile. In Fig. 4 examples of normalized VA plots from airgun shots are shown for OBS0104, OBS0107 and OBS0112. Traveltimes of water waves and waves in low velocity sediments (including multiples) are marked in blue. They are important for

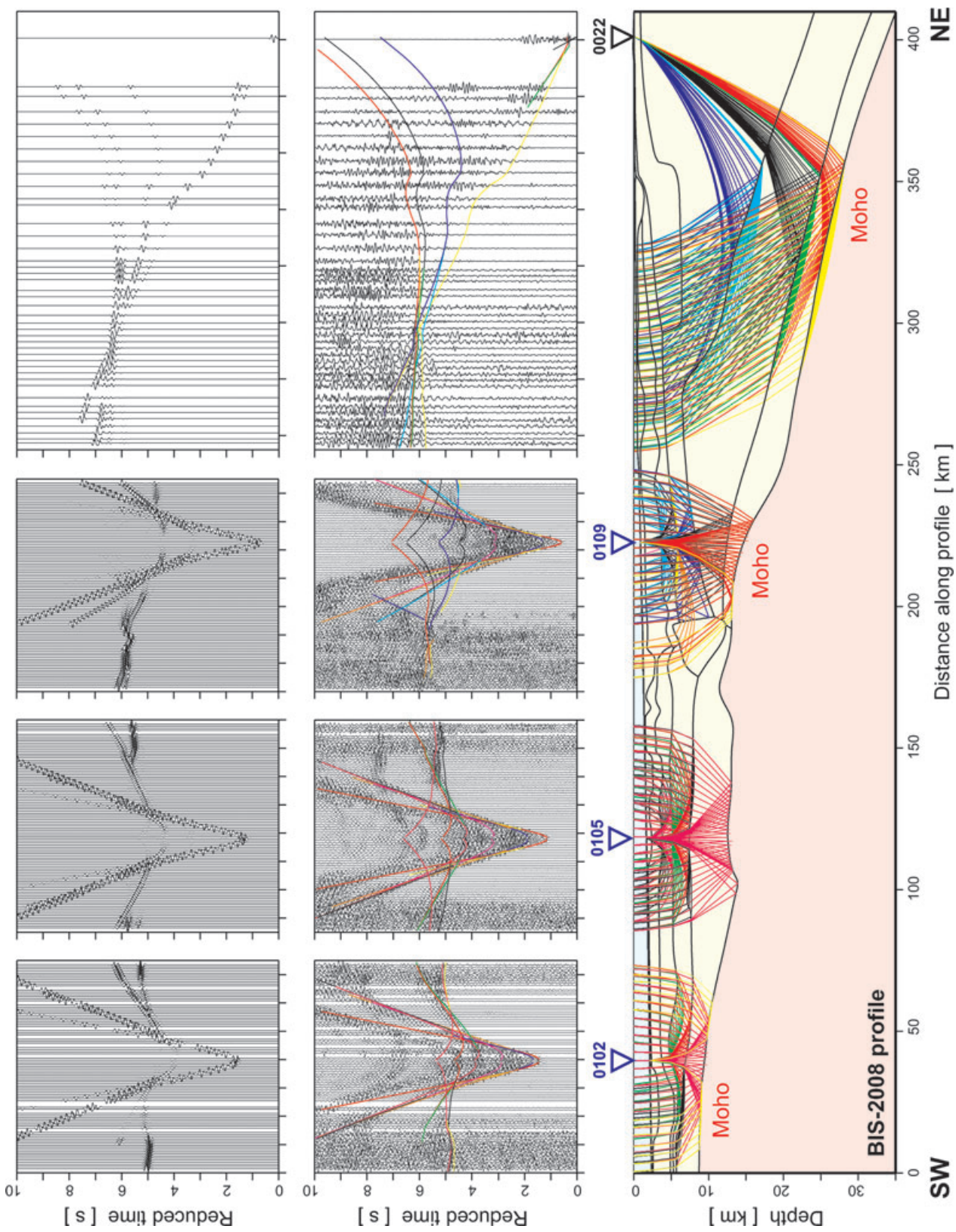

Figure 6. Example of the 2-D seismic modelling along BIS-2008 profile: model with rays (bottom), observed record sections (vertical-component) with calculated traveltimes (middle) and synthetic seismograms (top). Amplitude-normalized (WT plots) sections of airgun shots for OBS0102, OBS0105 and OBS0109 and section of chemical shots for land station 0022. Colours of calculated traveltimes correspond to ray colours in the ray diagram; only chosen rays are shown, related with deeper crust and Moho. Band-pass filtration is 3–17 Hz and velocity reduction 8 km s^{-1}.

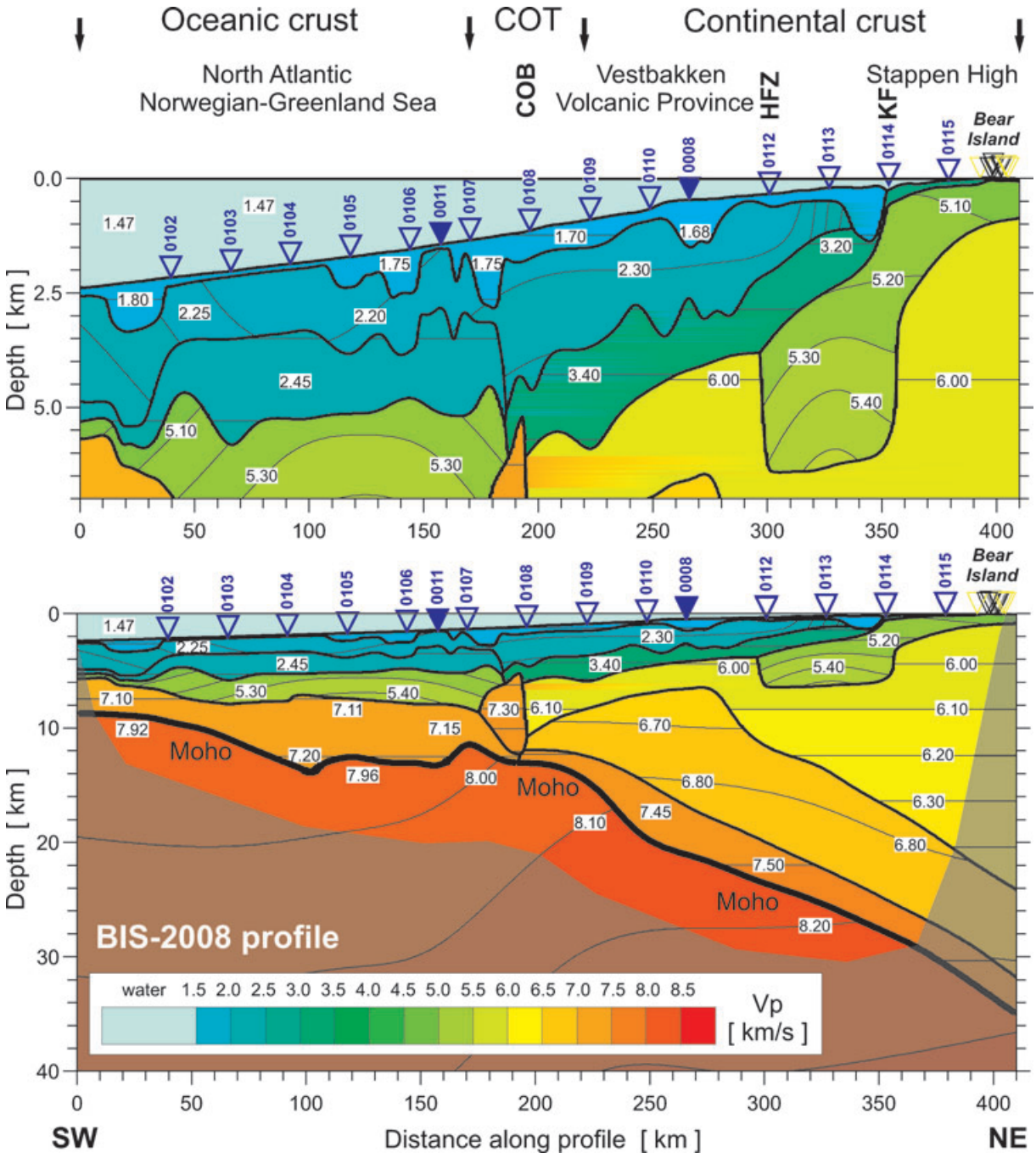

Figure 7. Two-dimensional seismic *P*-wave velocity model along the BIS-2008 profile developed by ray tracing technique. Upper diagram shows uppermost 7 km of the model with vertical exaggeration 20:1 and lower one shows the whole model with vertical exaggeration 5:1. Triangles show location of OBSs and land stations. Black lines represent seismic discontinuities (boundaries); coloures represent the distribution of the *P*-wave velocity and numbers in the model are *P*-wave velocities in km s^{-1}. Areas of missing ray coverage are marked by grey overlay.

sediment structure determination. Traveltimes of crustal *P*-waves and waves reflected and refracted from the Moho are marked in red. They are crucial for crustal structure determination. In the south-western part of the profile (OBS0104) because of deep ocean and shallow Moho, crustal phases are observed only in a very narrow offset range, 10–20 km from the OBS. For farther offset, refracted waves from the lower crust and Moho are observed, with apparent velocities close to 8 km s^{-1}. Waves reflected from Moho are observed in the 30–50 km offset range. A very complicated pattern of first arrivals is observed for OBS0107 to the northeast. It results from the shallow sedimentary structure as well as from the existence of high velocity rocks in the upper crust. In the northeastern part of the profile (OBS0112) with shallow water and thick crust, the crustal phases are observed to large offset, over 80 km, with apparent velocities about 6.5 km s^{-1}. Similar wave pattern is observed for land station and TNT shots (Figs 5 and 6). In Fig. 5 distant crustal and Pn phases are observed in 100–190 km offset range. In both sections we can distinguish three phases: Pn at distance 270–

300 km (with calculated traveltime line in yellow), middle crust phase at distance 250–290 km (with calculated traveltime line in blue) and lower crust high velocity phase at distance 210–260 km (with calculated traveltime line in red). Similar pattern can be observed for land station 0022 in Fig. 6.

Apart from the regular refracted and reflected phases we can observe, particularly at off-shore sections, distinct multiples. In Fig. 4 theoretical multiples (with one extra reflection in the water layer) are marked in green and they fit quite well the observed multiples. In the deep water they are clearly separated from direct waves, being later by *ca.* 2 s for OBS0104 and *ca.* 1.5 s for OBS0107. Another situation is observed for OBS0112 located in the shallow water. Here the time delay of multiples is *ca.* 0.8 s and we have a mixture of 'direct' (red) and 'multiples' (green). In all record sections we observe also double, triple and so multiples. Some of the observed phases are *S*-waves, converted P-to-S phase, with corresponding multiples. Correlation of deeper arrivals should thus be done very carefully in order not to mix 'direct phases' with 'multiples'. On the other hand, proper interpretation of multiples could be an additional verification for the correctness of the model.

DERIVATION OF 2-D CRUSTAL MODEL USING A RAY TRACING TECHNIQUE

Good quality data recorded along BIS-2008 profile permitted detailed 2-D forward modelling of all observed refracted, reflected and post-critical phases using the ray tracing technique. Identification and correlation of seismic phases were done manually on a computer screen using the ZPLOT software, which allows scaling, filtering and reduction velocity (Zelt 1994; Środa 1999). Computation of traveltimes, ray paths and synthetic seismograms were performed using the SEIS83 package (Červený & Pšenčík 1983) enhanced by employing the interactive graphical interfaces MODEL (Komminaho 1993). The initial model for 2-D modelling was the ocean water layer, which depth was profiling during the cruise. The sea bottom depth changes from about 2400 m in the SW end of profile, to about 1200 m at the continental–ocean transition. Elevations of the land stations were taken from GPS. The initial *P*-wave velocity for the water layer was assumed to be 1500 m s^{-1}, which was slightly changed during the modelling process. The final velocity value was in the range of 1460–1480 m s^{-1}, which represents typical sound speeds in the Norwegian-Greenland Sea (e.g. Mjelde *et al.* 2002). No multi-channel seismic data were available for constraining the sedimentary and upper crustal structure prior to modelling.

The 2-D velocity model for sediments, crystalline crust and crust–mantle transition was successively altered by trial and error. Traveltimes for the consecutive layers were recalculated many times until agreement was obtained between observed (picked) and model-derived traveltimes. Inaccuracy of the picking we evaluate to be of about 0.1 s. Simultaneously to kinematic modelling, synthetic seismograms were calculated to control velocity gradients within the layers and velocity contrasts across seismic boundaries. Examples of kinematic modelling are shown in Figs 4 and 5, where theoretical traveltimes were calculated for the final model of the structure shown in Fig. 7. Four examples of dynamic modelling are shown in Fig. 6, where amplitude-normalized sections (WT plots) of airgun shots for OBS0102, OBS0105 and OBS0109 and section of TNT shots for land station 0022 are compared with synthetic seismograms. The synthetic seismograms show good qualitative agreement with the relative amplitudes of observed refracted and reflected waves.

VELOCITY MODEL AND ITS ACCURACY

From the crustal structure point of view the whole profile could be divided into three parts: 0–170 km distance corresponding to oceanic crust and 220–410 km distance corresponding to continental crust. The depth of Moho reaches 8–13 km for the oceanic crust and 15–30 km for the continental crust. The continent–ocean transition occurs at 170–220 km distance, where the most complicated structure is observed, including a high velocity body (HVB) within the crust. Uppermost mantle velocities were determined from Pn waves: they change from 7.9–8.0 km s^{-1} beneath the oceanic crust to 8.1–8.2 km s^{-1} beneath the continental crust.

Oceanic domain

A layer of 100–1000 m thickness consisting of low velocity sediments were found along the whole profile length (with exception of Bear Island), with velocities of about 1.7–1.8 km s^{-1}. Two sedimentary layers of 1–2 km thickness with velocities of 2.2–2.3 and 2.4–2.5 km s^{-1} were found in this part of the profile. They reach a thickness of 3–3.5 km and are characterized by significant changes in topography. The largest variations in thickness are observed in the distance range 0–40 km in the southwestern end of the profile and in the distance range 110–170 km. Since constraints from multichannel seismic data are not available, the significance of this shallow structuring is unknown. Beneath these layers a 2–3 km thick layer with velocities of 5.2–5.4 km s^{-1} and a deeper 3–8 km thick lower crust with velocities of 7.1–7.2 km s^{-1} were found. They form near horizontal layering in the distance range 100–170 km, with significant thinning toward southwest, with the Moho at 9 km depth.

Continental domain

The uppermost low velocity sedimentary layer of about 100–1000 m thickness with velocities of about 1.7–1.8 km s^{-1} was found along the whole profile length (with exception of Bear Island). The first sedimentary layer in the continental part of the profile has almost the same properties as for the oceanic part: about 2 km thick with velocities of 2.25–2.4 km s^{-1}. However, its structuring is not as complex as for the oceanic part. The second 1–2 km thick layer has velocities 3.2–3.4 km s^{-1}, which are much higher compared to the oceanic part of the profile. In the northeastern part of the profile (300–410 km) 5.1–5.5 km s^{-1} velocities were found beneath the sedimentary complex, similar to those found for the oceanic crust. Beneath the uppermost layers three layers were found which build the crystalline complex of the continental crust. Two of them are totally different from those of the oceanic crust. Their velocities are 6.0–6.3 and 6.65–6.85 km s^{-1} and their thicknesses are up to 15 and 10 km, respectively. The third layer is more similar to the lower oceanic crust, however the velocity is significantly higher; 7.4–7.55 km s^{-1}. Lowering this velocity of 0.4 km s^{-1} causes delay in time of about 1 s. This part of the crust is also much thicker and Moho is nearly smoothly deepening from about 14 km at 220 km of the profile, to about 30 km at a distance of 370 km. The Moho is not illuminated by rays, so the Moho depth is not constrained for the easternmost 40 km of the model. Comparison with other results from the Barents Sea (south of Bear Island) suggests that the Moho along this part of the profile most likely would be about 28–32 km deep (Mjelde *et al.* 2002).

HVB at COT

The model shows the most complex structures between 170 and 220 km model distance, in the transition between oceanic and continental crust. The elements of the oceanic and continental crust within this zone are disturbed and deformed and its central part is occupied by a HVB, with velocities of 7.2–7.4 km s^{-1}. The top of this body reaches a depth of about 6 km, while its bottom is at about 12 km depth. The body is 10–20 km wide and occupies the entire crystalline portion of the crust. Taking into account the shallow location of the HVB, its velocity is significantly higher then the velocity in the lower oceanic crust. The velocity in the HVB was determined mainly from refracted waves observed at OBS0107 (Fig. 4 middle). It is also observed as a far distance reflected phase from the 'right side' of HVB recorded at OBS0109 (in Fig. 6 violet branch of traveltime and corresponding rays).

Model accuracy

Because of offshore location of the profile all shots (airgun and TNT) and receivers (OBSs) were in-line (Fig. 2). Only some of the land stations were off the profile line, however this deviation is small and does not exceed 10 km (see insert in Fig. 2). Using modern GPS techniques, the shot times and locations for shots and receivers were measured very precisely, on the order of 1 ms and tens of meters, respectively. Such errors are insignificant in a crustal-scale experiment. Uncertainties of velocity and depth in the model obtained using the ray tracing technique result first of all from the uncertainties of subjectively pickedtraveltimes, which is in the order of 0.1 s. However, the accuracy increases with increasing quality and amount of data (number of shots and receivers, effectiveness of sources, signal-to-noise ratio, reciprocity of traveltime branches, ray coverage in the model). In the offshore experiments additional complications are due to the water-multiples, multiples of *P*- and *S*-waves and converted *P*-to-*S* waves. When interpreted incorrectly, they can lead to serious mistakes, which cannot be estimated. Our final model of the structure explains however both 'direct waves' as well as 'multiples'.

In case of good quality of data and interpretation the use of ray tracing produced theoretical traveltimes that fitted the observed (experimental) traveltimes for both refracted and reflected waves with good accuracy. The Moho depth accuracy is of the order 1 km for the oceanic crust and about 2 km for the continental crust. (see e.g. Janik *et al.* 2002; Mjelde *et al.* 2002; Grad *et al.* 2003, 2006, 2008; Środa *et al.* 2006). Diagrams showing theoretical and observed traveltimes for all the phases along the profile, ray coverage and traveltime residuals from forward modelling are shown in Fig. 8. There is visible very good agreement with some not important exceptions. The continental crust is better determined than oceanic and transition part of the model (ray coverage, Fig. 8b) because of existence of many land stations in the Bear Island. Anyway, even some almost vertical boundaries are well imaged from reflections. Others are determined using refracted-waves which is with less accuracy but because of clearly visible changes in the wave field during modelling, the accuracy is up to 5 km horizontally. RMS values are even better than presumptions, being 0.12 for sediments, 0.09 for the crust and 0.08 for PmP and 0.07 for Pn phases. The overall RMS value is 0.094 from 17 805 picks.

DISCUSSION

Shallow sedimentary section

The modelled profile crosses the Bear Island fan, known as a major glacial, Plio-Pleistocene depositional centre (e.g. Solheim *et al.* 1998). The glaciations started at *ca.* 3.6 Ma, between 2.4 Ma and 1.0 Ma the Barents Sea ice sheet developed to a moderate size and after 1.0 Ma repeated ice sheet advances to the shelf edge occurred (Knies *et al.* 2009). The sediments were deposited as glacigenic debris flows, modified by contourites and gravitational instabilities (e.g Solheim *et al.* 1998). Earlier studies involving shallow drillholes and multichannel seismic data have shown that the *P*-wave velocities in the glacigenic fan varies with depth from *ca.* 1.6 to 2.5 km s^{-1} (Faleide *et al.* 1988). We thus interpret the uppermost two layers in our model (*ca.* 1.8 km s^{-1} and *ca.* 2.3 km s^{-1}) as dominantly being part of the Plio-Pleistocene glacigenic fan. It is likely that the deepest portion of the 2.3 km s^{-1} layer northeast-ward of the COB represents Late Eocene-Miocene sediments and that the deepest portion of the 2.45 km s^{-1} layer southwest-ward of the COB corresponds to Miocene sediments. The thickness of the Plio-Pleistocene wedge cannot be resolved by our data.

Continental crust (220–410 km)

P-wave velocities as low as 3–3.5 km s^{-1} within the Vestbakken volcanics have been reported from shallow drillholes (Faleide *et al.* 1988). This corresponds well to the *ca.* 1.5 km thick 3.2–3.5 km s^{-1} layer in our model between the COB and the Knølegga Fault. The velocities are 1–1.5 km s^{-1} lower than usually found on volcanic margins (e.g. Mjelde *et al.* 2005), indicating that the layer consists of a mixture of volcanic flows, tuffs and sedimentary units.

A 3–4 km thick sedimentary basin beneath the volcanics is modelled between the HFZ and the KF. The *P*-wave velocity within the layer varies with depth from *ca.* 5.1 to 5.5 km s^{-1}. Permian/Carboniferous sedimentary rocks outcrop on the seafloor near the northeastern termination of the profile (Faleide *et al.* 1988). These outcropping rocks have velocities slightly above 5.0 km s^{-1} and we thus interpret the layer as being dominantly of Permian/Carboniferous age. It cannot be excluded that the uppermost 1–2 km of the layer represents Jurassic-Cretaceous sedimentary units southwest-ward of KF. Note that our model suggests that the HFZ is located *ca.* 20 km southwest-ward of the location inferred earlier from interpretation of multichannel seismic data (Fig. 1; Faleide *et al.* 1988), whereas our location of KF agrees well with earlier interpretations.

The crystalline crust is modelled as three layers with *P*-wave velocities of 6.0–6.4 km s^{-1}, 6.7–6.8 km s^{-1} and 7.5 km s^{-1}, respectively. The velocities in the uppermost two layers are typical for granitic/granodioritic continental crust (e.g. Mjelde *et al.* 2002). However, the *P*-wave velocity in the 3–4 km thick lowermost crust is significantly higher than normal. Lowering the velocity in this layer of 0.4 km s^{-1} causes delay in time of about 1 s during test modelling. It is unlikely that the layer represents serpentinized peridotites, taking into account results from neighbouring area (Mjelde *et al.* 2009). The crystalline crust is rather thick and there is no evidence of fractures in the crust similar to those found for example, by Edwards *et al.* (1997). We interpret the layer as a mixture of mafic intrusions and continental crystalline blocks, similar to the current models applied for the outer mid-Norwegian margin (e.g.

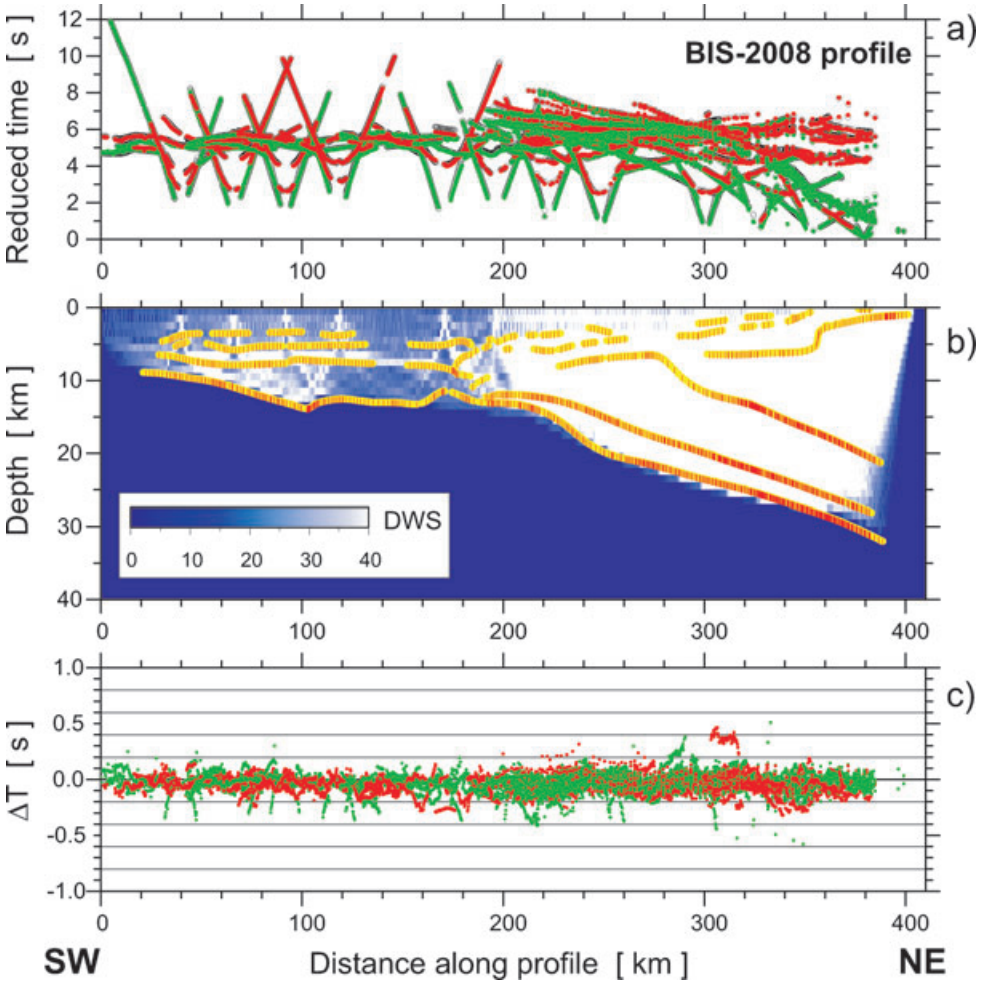

Figure 8. Diagrams showing theoretical and observed traveltimes (a), ray coverage (b) and traveltime residuals (c) from forward modelling along the profile BIS-2008. Green points—refracted arrivals, red points—reflections, black circles—theoretical traveltimes. Yellow lines—fragments of discontinuities constrained by reflected phases. The red points plotted along the interfaces mark the bottoming points of the modelled reflected phases (every third point is plotted) and their density is a measure of the positioning accuracy of the reflectors.

Mjelde *et al.* 2009). According to this model, the higher velocity is due to increased Mg content in the melt caused by higher than normal temperature in the mantle (White & McKenzie 1989).

We note that the Paleozoic-Mesozoic thinning was localized within the upper crystalline crust, whereas the thinning southwestward of the HFZ was strongly concentrated within the lower crustal 6.7–6.8 km s^{-1} layer. We infer this difference to lower crustal heat softening during the Paleocene-Early Eocene phase of rifting. The rifting was accompanied by mafic intrusions in the lowermost crust and volcanic activity forming the main part of the Vestbakken Volcanic Province. Since Early Eocene influence from the Iceland Plume has been inferred as far north as the SFZ (Mjelde *et al.* 2008), we suggest that the higher temperatures needed to cause the lower crustal intrusions along our profile were related to the Icelandic Plume. However, it must be emphasized that it cannot be excluded that the excess magmatism can be related to non-plume mechanisms (Mjelde *et al.* 2009).

Oceanic crust (0–170 km)

The *P*-wave velocities in the crystalline portion of the crust in the model range 0–170 km are typical for oceanic crust; the 5.2–5.4 km s^{-1} layer being oceanic layer 2 (pillow lavas and feeder dikes) and the 7.1–7.2 km s^{-1} layer representing oceanic layer 3 (gabbroic complex). The part of the crust northeast-ward of 90 km has been accreted along the Knipovich Ridge from continental break-up at *ca.* 35 Ma until *ca.* 20 Ma. The average thickness of the magmatic portion of the crust is here 8 km. Taking into account that the spreading was ultra slow, this is 3–5 km thicker than normal (White *et al.* 1992; Kandilarov *et al.* 2008). It is unlikely that the increased magmatism and thereby enhanced thickness of the crust can be attributed to influence from the Icelandic Plume, as its activity in this period was low (Mjelde *et al.* 2008). Instead we interpret the increased magmatism as a passive response to the (extensional) bending of this southernmost part of the Knipovich Ridge.

The part of the model southwest-ward of 90 km is roughly parallel to Mohns Ridge and represents oceanic crust formed at *ca.* 20 Ma. The thickness of the magmatic portion of the crust decreases southwest-wards to *ca.* 3 km, which is normal for ultra slow spreading ridges (Klingelhöfer *et al.* 2000a,b). The normal thickness of the crust along this part of the Mohns Ridge, strongly suggest that the larger thickness of the crust formed along the southernmost part of the Knipovich Ridge was unrelated to influence from the Icelandic Plume.

The continent–ocean-transition (170–220 km)

The crystalline portion of the crust within the south-western part of the COT consists of a *ca.* 30 km wide and *ca.* 6 km thick high-velocity (7.3 km s^{-1}) body. The body has similarities to the core of oceanic plateaus formed at volcanic margins, for example, the Vøring Plateau (Mjelde *et al.* 2005). However, it is unlikely that the body represents mafic rocks emplaced during and immediately after break-up, since such high-temperature processes normally form oceanic crust significantly thicker than normal, for example, 23 km for the Vøring Plateau. Furthermore, the high-velocity bodies formed at volcanic margins are generally overlain by a significant extrusive complex with *P*-wave velocity around 4–5 km s^{-1}, which is not found in our area.

Instead we interpret the high-velocity body as serpentinized peridotites, that is, exhumed mantle. Such bodies are commonly observed within the COT along non-volcanic margins, characterized by slow continental extension followed by slow oceanic spreading (e.g. Minshull 2009). This interpretation implies that continental break-up occurred somewhat earlier than the plate change at *ca.* 35 Ma, which caused increased extension, magmatism and thickness of the oceanic crust. Furthermore, it implies that the formation of the Vestbakken Volcanic Province (with intrusions in the lower crust) was dominantly restricted to the Paleocene-Early Eocene event.

Based on the modelled *P*-wave velocity, we interpret the part of the crust in the range 200–220 km as strongly thinned continental crust. We include this portion within the COT, as the model is not well resolved here. We define the north-eastern termination of the high-velocity body as the Continent–Ocean-Boundary (COB) and note that this location is *ca.* 10 km southwest-ward of earlier interpretations (Fig. 2; Breivik *et al.* 1999).

The *P*-wave velocity in the upper mantle is modelled to decrease gradually south-westwards from *ca.* 8.2 to 7.9 km s^{-1}. Such velocity changes are common across passive margins (e.g. mid-Norway; Mjelde *et al.* 2005). Along our profile, however, the velocity variation may be pressure induced, since the Moho drops from 10 to 14 km in the southwest to *ca.* 30 km beneath the Bear Island. Note that the Moho beneath the high-velocity body located within the COT does not correspond to the top of the mantle.

Other profiles from the vicinity of the study area (Mjelde *et al.* 2002; Breivik *et al.* 2003; Ljones *et al.* 2004) show a very abrupt COT landward of normal, ultra-slow spreading oceanic crust. A similar abrupt COT is found by Edwards *et al.* (1997) and Greenroyd *et al.* (2008) at the margin off Ghana and French Guiana, respectively. Our studied margin segment is wider, with a HVB (7.5 km s^{-1}) in the lower crust. This crustal structure is consistent with a combination of shearing and rifting forming a trans-tensional margin segment, influenced by magmatism related to the Icelandic Plume. Shearing is confined mostly to the HFZ, whereas evidence of extension is more widespread, from the HFZ to the COB (Faleide *et al.* 1991, 2008).

CONCLUSIONS

The *P*-waves observed in a 410 km long OBS profile from the Bear Island, Barents Sea to oceanic crust formed along the Mohns Ridge have been modelled by use of kinematic and dynamic ray-tracing. The modelling confirms the effectiveness of the acquisition set-up: short-period recorders, a dense system of the air-gun shots in the thin oceanic crust area and TNT shots for recognition of the thick continental crust.

The northeastern part of the model represents typical continental crust, thinned from *ca.* 30 km thickness beneath the Bear Island to *ca.* 13 km within the COT. The shallowest 3–4 km of the sediments along the continental slope dominantly represents Plio-Pleistocene glasigenic deposits. This wedge is underlain by a *ca.* 1.5 km thick layer of volcanics, known as the Vestbakken Volcanic Province. A 3–4 km thick sedimentary basin beneath the volcanics is modelled between the HFZ and the KF. The *P*-wave velocity within the layer varies with depths from *ca.* 5.1 to 5.5 km s^{-1}, suggesting dominantly Permian/Carboniferous age. The *P*-wave velocity in the 3–4 km thick lowermost continental crust is significantly higher than normal (*ca.* 7.5 km s^{-1}). We interpret this layer as a mixture of mafic intrusions and continental crystalline blocks, dominantly related to the Paleocene-Early Eocene event.

The crystalline portion of the crust within the south-western part of the COT consists of a *ca.* 30 km wide and *ca.* 6 km thick high-velocity (7.3 km s^{-1}) body. We interpret the body as serpentinized peridotites, that is, exhumed mantle. The magmatic portion of the ocean crust accreted along the Knipovich Ridge from continental break-up at *ca.* 35 Ma until *ca.* 20 Ma has an average thickness of 8 km, which is 3–5 km thicker than normal. We interpret the increased magmatism as a passive response to the (extensional) bending of this southernmost part of the Knipovich Ridge. The thickness of the magmatic portion of the crust formed along the Mohns Ridge at *ca.* 20 Ma decreases gradually to *ca.* 3 km, which is normal for ultra slow spreading ridges. The normal thickness of the crust along this part of the Mohns Ridge, strongly suggest that the larger thickness of the crust formed along the southernmost part of the Knipovich Ridge was unrelated to influence from the Icelandic Plume.

Our preferred model is thus:

(1) Early Eocene trans-tensional, leaky transform, influenced by the Icelandic Plume (Raum *et al.* 2006). Formation of the high velocity layer in the lower crust.

(2) Continued shear along the HFZ but with non-magmatic rifting until break-up, exhumation of mantle and formation of the serpentinized peridodites.

(3) Renewed extension (due to the bend in the spreading ridge) while oceanic crust is being formed. More magmatism than normal.

(4) Western end of the profile, south of the bend in the spreading ridge: normal, ultra-slow spreading.

ACKNOWLEDGMENTS

IPY-Project Group comprises: J. Schweitzer (Norsar), R. Mjelde (University of Bergen), F. Krüger (University of Potsdam), A. Guterch (Polish Academy of Sciences), M. Schmidt-Aursch (Alfred Wegener Institute), M. Grad (University of Warsaw), J.I. Faleide (University of Oslo). The paper was done in the framework of the 4th International Polar Year Panel 'Plate Tectonics and Polar Gateways', the international project 'The Dynamic Continental Margin Between the Mid-Atlantic-Ridge System (Mohns Ridge, Knipovich Ridge) and the Bear Island Region'. The experiment was financed by the Norwegian Research Council (NFR Project number 176069/S30), PGNiG (Polish Oil and Gas Company SA) and Ministry of Science and Higher Education in Poland. The authors thank to University of Bergen for the short period OBS data and air-gun shooting, Institute of Geophysics PAS and Warsaw University for short-period land stations data and TNT shooting, University of Potsdam and NORSAR for Bjørnøya Array data and Alfred-Wegener Institute for the DEPAS data. The public domain GMT

software (Wessel and Smith 1991, 1998) has been used to produce maps.

REFERENCES

Birkenmajer, K., 1981. The geology of Svalbard, the western part of Barents Sea and the continental margin of Scandinavia, in *The Ocean Basins and Margins,* The Arctic Ocean, Vol. 5, pp. 265–239, eds. Nairn, A.E., Churkin, M., Jr., & Stehli, F.G., Plenum, New York.

Breivik, A.J., Mjelde, R., Grogan, P., Shimamura, H., Murai, Y. & Nishimura, Y., 2003. Crustal structure and transform margin development south of Svalbard based on ocean bottom seismometer data, *Tectonophysics,* **369,** 37–70.

Breivik, A.J., Verhoef, J. & Faleide, J.I., 1999. Effect of thermal contrasts on gravity modeling at passive margins: results from the western Barents Sea, *J. geophys. Res.,* **104,** 15293–15311.

Červený, V. & Pšenčík, I., 1983. 2-D seismic ray tracing package SEIS83 (software package), Charles University, Prague.

Crane, K., Sundvor, E., Buck, R. & Martinez, F., 1991. Rifting in the northern Norwegian-Greenland Sea: thermal tests of asymmetric spreading, *J. geophys. Res.,* **96,** 14529–14550.

Czuba, W., *et al*. 2008. Seismic crustal structure along the deep transect Horsted'05, Svalbard, *Pol. Polar Res.,* **29**(3), 279–290.

Davydova, N.I., Pavlenkova, N.I., Tulina, YU.V. & Zverev, S.M., 1985. Crustal structure of the Barents Sea from seismic data, *Tectonophysics,* **114,** 213–231.

Døssing, A., Dahl-Jensen, T., Thybo, H., Mjelde, R. & Nishimura, Y., 2008. The East Greenland Ridge in the North Atlantic: an integrated geophysical study of a continental sliver in a transform fault setting, *J. geophys. Res.,* **113,** B10107, doi:10.1029/2007JB005536.

Edwards, R.A., Whitmarsh, R.B. & Scrutton, R.A., 1997. The crustal structure across the transform continental margin off Ghana, eastern equatorial Atlantic, *J. geophys. Res.,* **102**(B1), 747–772.

Eiken, O. & Austegard, A., 1987. The Tertiary orogenic belt of West Spitsbergen: seismic expressions of the offshore sedimentary basins, *Nor. Geol. Tidsskr.,* **67,** 383–394.

Eldholm, O., Faleide, J.I. & Myhre, A.M., 1987. Continental-ocean transition at the western Barents Sea/Svalbard continental margin, *Geology,* **15,** 1118–1122.

Faleide, J.I., Myhre, A.M. & Eldholm, O., 1988. Early Tertiary volcanism at the western Barents Sea margin, *Geol. Soc. Lond. Spec. Publ.,* **39,** 135–146.

Faleide, J.I., Gudlaugsson, S.T., Eldholm, O., Myhre, A.M. & Jackson, H.R., 1991. Deep seismic transects across the western Barents Sea continental margin, *Tectonophysics,* **189,** 73–89.

Faleide, J.I., Tsikalas, F., Breivik, A.J., Mjelde, R., Ritzmann, O., Engen, Ø., Wilson, J. & Eldholm, O., 2008. Structure and evolution of the continental margin off Norway and the Barents Sea, *Episodes* **31(1)**, 82–91.

Gabrielsen, R.H., Færseth, R.B., Jensen, L.N., Kalheim, J.E. & Riis, F., 1990. Structural elements of the Norwegian continental shelf, Part I: the Barents Sea Region, *NPD-Bulletin No 6*, 1–33, Oljedirektoratet.

Gjelberg, J., 1981. Upper Devonian (Famennian) – Middle Carboniferous succession of Bjørnøya, *Norsk Polarinstitutt Skrifter,* **174,** 1–67.

Gjelberg, J., 1987. Early Carboniferous graben style and sedimentation response, Svalbard, in *European Dinantian environments,* pp. 93–113, eds. Miller, J., Adams, A.E. & Wright, V.P., John Wiley & Sons Ltd, Chichester.

Grad, M., *et al*. 2003. Crustal structure of the Trans-European suture zone region along POLONAISE'97 seismic profile P4, *J. geophys. Res.,* **108**(B11), 2541, doi: 10.1029/2003JB002426.

Grad, M., *et al*. 2006. Lithospheric structure beneath trans-Carpathian transect from Precambrian platform to Pannonian basin: CELEBRATION 2000 seismic profile CEL005, *J. geophys. Res.,* **111,** B03301, doi: 10.1029/2005JB003647.

Grad, M., Guterch, A., Mazur, Z., Keller, G.R., Špičák, A., Hrubcová, P. & Geissler, W.H., 2008. Lithospheric structure of the Bohemian Massif and adjacent Variscan belt in central Europe based on profile S01 from the SUDETES 2003 experiment, *J. geophys. Res.,* **113,** B10304, doi:10.1029/2007JB005497.

Greenroyd, C.J., Peirce, C., Rodger, M., Watts, A.B. & Hobbs, W., 2008. Demerara Plateau – the structure and evolution of a transform passive margin, *Geophys. J. Int.,* **172,** 549–564, doi: 10.1111/j.1365-246X.2007.03662.x.

Jakobsson, M., Cherkis, N.Z., Woodward, J., Macnab, R. & Coakley, B., 2000. New grid of Arctic bathymetry aids scientists and mapmakers, *EOS, Trans. AGU,* **81**(9), 89, 93, 96.

Janik, T., Yliniemi, J., Grad, M., Thybo, H., Tiira, T. & POLONAISE P2 Working Group, 2002. Crustal structure across the TESZ along POLONAISE '97 seismic profile P2 in NW Poland, *Tectonophysics,* **360,** 129–152.

Kandilarov, A., Mjelde, R., Okino, K. & Murai, Y. 2008. Crustal structure of the ultra slow spreading Knipovich Ridge, North Atlantic, derived from OBS, MCS and gravity data, along a presumed amagmatic portion of crustal formation, *Mar. Geophys. Res.,* **29,** 109–134, doi: 10.1007/s11001-008-9050-0.

Klingelhöfer, F., Géli, L. & White, R.S., 2000a. Geophysical and geochemical constraints on crustal accretion at the very-slow spreading Mohns Ridge, *Geophys. Res. Lett.,* **27**(10), 1547–1550.

Klingelhöfer, F., Géli, L., Matias, L., Steinsland, N. & Mohr, J., 2000b. Crustal structure of a super-slow spreading centre: a seismic refraction study of Mohns Ridge, 72°N, *Geophys. J. Int.,* **141,** 509–526.

Knies, J., *et al*. 2009. A new Plio-Pleistocene ice sheet model for the Svalbard/Barents Sea region. *Quat. Sci. Rev.,* **28,** 812–829.

Komminaho, K., 1993. Software manual for programs MODEL and XRAYS–a graphical interface for SEIS83 program package, University of Oulu, Department of Geophysics, Report No. 20, p. 31.

Ljones, F., Kuwano, A., Mjelde, R., Breivik, A., Shimamura, H., Murai, Y. & Nishimura, Y., 2004. Crustal transect from the North Atlantic Knipovich Ridge to the Svalbard Margin west of Hornsund, *Tectonophysics,* **378,** 17–41.

Lundin, E. & Doré, A.G., 2002. Mid-Cenozoic post break-up deformation in the "passive" margins bordering the Norwegian-Greenland Sea, *Mar. Petroleum Geol,* **19,** 79–93.

Minshull, T.A. 2009. Geophysical characterisation of the ocean–continent transition at magma-poor rifted margins, *C.R. Geoscience,* **341,** 382–393.

Mjelde, R., *et al*. 2002. Geological development of the Sørvestsnaget Basin, SW Barents Sea, from ocean bottom seismic, surface seismic and potential field data, *Norwegian J. Geol.,* **82,** 183–202.

Mjelde, R., Breivik, A.J., Raum, T., Mittelstaedt, E., Ito, G. & Faleide, J.I. 2008. Magmatic and tectonic evolution of the North Atlantic, *J. Geol. Soc.,* **165,** 31–42.

Mjelde, R., Faleide, J.I., Breivik, A.J. & Raum, T., 2009. Lower crustal composition and crustal lineaments on the Vøring Margin, NE Atlantic: a review, *Tectonophysics,* **472**(1–4), 183–193.

Mjelde, R., Raum, T., Myhren, B., Shimamura, H., Murai, Y., Takanami, T., Karpuz, R. & Næss, U., 2005. Continent-Ocean-Transition on the Vøring Plateau, NE Atlantic, derived from densely sampled OBS-data, *J. geophys. Res.,* **110,** B05101, 1–19.

Mosar, J., Eide, E.A., Osmundsen, P.T., Sommarunga, A. & Torsvik, T.H., 2002. Greenland-Norway separation: a geodynamic model for the North Atlantic, *Norwegian J. Geol.,* **82/4,** 282–299.

Myhre, A.M., Eldholm, O. & Sundvor, E., 1982. The margin between Senja and Spitsbergen Fracture Zones: implications from plate tectonics, *Tectonophysics,* **89,** 33–50.

Pirli, M., *et al*. 2010. Preliminary Analysis of the 21 February 2008, Svalbard (Norway), Seismic Sequence, *Seism. Res. Lett.,* **81,** 63–72.

Raum, T., Mjelde, R., Shimamura, H., Murai, Y., Bråstein, E., Karpuz, R.M., Kravik, K. & Kolstø, H.J., 2006. Crustal structure and evolution of the southern Vøring Basin and Vøring Transform Margin, NE Atlantic, *Tectonophysics,* **415,** 167–202.

Schweitzer, J., Guterch, A., Krüger, F., Schmidt-Aursch, M., Mjelde, R., Grad, M. & Faleide, J., 2008. The IPY Project 77 – The dynamic continental margin between the Mid-Atlantic-Ridge system (Mohns Ridge, Knipovich Ridge) and the Bear Island Region, in *Proceedings of the 33 International Geological Congress,* Oslo, 6–14 August 2008, CD-ROM Proceedings.

Sellevoll, M.A., Duda, S.J., Guterch, A., Pajchel, J., Perchuć, E. & Tyssen, F., 1991. Crustal structure in the Svalbard region from seismic measurements, *Tectonophyics,* **189,** 55–71.

Solheim, A., *et al*. 1998. Late Cenozoic seismic stratigraphy and glacial geological development of the East Greenland and Svalbard–Barents Sea continental margins. *Quat. Sci. Rev.,* **17,** 155–184.

Środa, P., 1999. Modification to software package ZPLOT by C. Zelt.

Środa, P., *et al.* & CELEBRATION 2000 Working Group, 2006. Crustal and upper mantle structure of the Western Carpathians form CELEBRATION 2000 profiles CEL01 and CEL04: seismic models and geological implications, *Geophys. J. Int.,* **167,** 737–760.

Sundvor, E. & Eldholm, O., 1979. The western and northern margin off Svalbard, *Tectonophysics,* **59,** 239–250.

Talwani, M. & Eldholm, O., 1977. The evolution of the Norwegian-Greenland Sea: recent results and outstanding problems, *Geol. Soc. Am. Bull.,* **88,** 969–999.

Vogt, P.R., Perry, R.K., Feden, R.H., Fleming, H.S. & Cherkis, N.Z., 1981. The Greenland-Norwegian Sea and Iceland environment: geology and geophysics, in *The Arctic Ocean. The Ocean Basins and Margins,* Vol. 5, pp. 493–598, eds. Nairn, A.E.M., Churkin, M.C. Jr. & Stehli, F.G., Plenum Press, New York, NY.

Wessel, P. & Smith, W.H.F., 1991. Free software helps map and display data, *EOS, Trans. AGU,* **72,** 441.

Wessel, P. & Smith, W.H.F., 1998. New, improved version of the Generic Mapping Tools released, *EOS, Trans. AGU,* **79,** 579.

White, R.S. & McKenzie, D., 1989. Magmatism at rift zones: the generation of volcanic continental margins and flood basalts, *J. geophys. Res.,* **94,** 7685–7729.

White, R.S., McKenzie, D. & O'Nions, R.K., 1992. Oceanic crustal thickness from seismic measurements and rare earth element inversions, *J. geophys. Res.,* **97,** 19683–19715.

Wilde-Piórko, M., Grad, M., Wiejacz, P., & Schweitzer, J., 2009. HSPB seismic broadband station in Southern Spitsbergen: first results on crustal and mantle structure from receiver functions and SKS splitting, *Pol. Polar Res.,* **30**(4), 301–316.

Zelt, C.A., 1994. Software package ZPLOT. Bullard Laboratories, University of Cambridge, Cambridge.